

INTERACTION BETWEEN AN UPSTREAM
FACING WALL JET AND A SUPERSONIC STREAM

Renzo Piva

January 25, 1972

(NASA-CR-112165) INTERACTION BETWEEN AN
UPSTREAM FACING WALL JET AND A SUPERSONIC
STREAM R. Piva (New York Univ.) 25 Jan.
1972 36 p

CSSL 20D

N72-30276

Unclas

G3/12 40026

Backup Document for AIAA Synoptic Scheduled
for Publication in the AIAA Journal, January 1973

New York University Aerospace Laboratory
New York University
School of Engineering and Science
University Heights, Bronx, N. Y. 10453

I

SYNOPTIC BACKUP DOCUMENT

This document is made publicly available through the NASA scientific and technical information system as a service to readers of the corresponding "Synoptic" which is scheduled for publication in the following (checked) technical journal of the American Institute of Aeronautics and Astronautics.

- AIAA Journal, January 1973
- Journal of Aircraft
- Journal of Spacecraft & Rockets
- Journal of Hydronautics

A Synoptic is a brief journal article that presents the key results of an investigation in text, tabular, and graphical form. It is neither a long abstract nor a condensation of a full length paper, but is written by the authors with the specific purpose of presenting essential information in an easily assimilated manner. It is editorially and technically reviewed for publication just as is any manuscript submission. The author must, however, also submit a full backup paper to aid the editors and reviewers in their evaluation of the synoptic. The backup paper, which may be an original manuscript or a research report, is not required to conform to AIAA manuscript rules.

For the benefit of readers of the Synoptic who may wish to refer to this backup document, it is made available in this microfiche (or facsimile) form without editorial or makeup changes.

II

INTERACTION BETWEEN AN UPSTREAM FACING WALL JET AND A SUPERSONIC STREAM*

by

Renzo Piva†

JANUARY 1972

* The work reported herein was supported by the National Aeronautics and Space Administration, under Grant No. NGR-33-016-131.

† Visiting Adjunct Professor, New York University Aerospace Laboratory
(Assistant Professor of Aerodynamics, University of Rome, Italy)

III

NOMENCLATURE

f	nondimensional stream function.....
g	temperature ratio
H	total enthalpy
L	distance of the step from the leading edge
l	step height
M	Mach number
p	pressure
s	injection slot height
T	temperature
U	velocity
u	x-component of velocity
v	y-component of velocity
γ	cooling effectiveness
ϵ	eddy viscosity
η	similar variable
λ	mass flow ratio = $\frac{\rho_j U_j}{\rho_e U_e}$
ρ	density
σ	angle of the shock
χ	coordinate defined in (1)
ψ	stream function

Subscripts

j	jet conditions
∞	infinite conditions
e	external conditions

ad adiabatic
w wall
o stagnation

LIST OF FIGURES

FIGURE

- 1a Shadowgraph pictures: Subsonic Injection
- 1b Flow field produced by upstream injection along the wall: subsonic injection
- 2a Shadowgraph pictures: Supersonic Injection
- 2b Flow field produced by upstream injection along the wall: Supersonic Injection
- 3 Experimental model
- 4 Deacription of the measured quantities along the wall between the leading edge and the injection slot: subsonic injection
- 5 Distribution of the measured quantities along the wall between the leading edge and the injection slot: supersonic injection
- 6 Measured quantities indicative of jet penetration and interaction, vs. jet Mach number
- 7 Cooling effectiveness correlation
- 8 Similar solution; nondimensional velocity profiles
- 9 Similar solution; nondimensional normal velocity profiles
- 10 Similar solution; nondimensional stream function profiles
- 11 Locally similar solution
- 12 Comparison of theoretical and experimental cooling effectiveness

ABSTRACT

The flow field resulting from the interaction of an upstream facing wall jet with a supersonic counterflowing stream has been investigated. A flow field model and the main parameters governing the phenomena were determined from quantitative and qualitative experimental observations. Experimental results for different ranges of the main parameters are presented. A theoretical analysis was performed to describe the flow field in the mixing region between the two counterflowing streams. The results obtained by applying a locally similar solution compare favorably with the experimentally measured values. Large values of jet penetration were obtained with a high subsonic or low supersonic jet; large interaction forces are characteristic of higher supersonic injections. For the case of large penetration the cooling effectiveness presented as a function of the main parameters indicates the possibility of interacting cooling applications.

VII

I. INTRODUCTION

The interaction of an upstream facing wall jet with a hypersonic counter-flowing stream gives rise to a complex flow field. The description of this flow field is interesting for the general understanding of complex interaction problems and for possible engineering applications. The injected gas penetrates upstream and then reverses interacting with the mainstream flow. A high mixing rate between the two counterflowing streams is characteristic of this flow field. Depending on the issuing jet conditions, different degrees of penetration and interaction can take place with correspondingly greatly diverse flow field structures.

Different technical applications can be appropriate to the various cases, in particular, the large jet penetrations is attractive for cooling problems, the high mixing rate for combustion problems, and large interaction forces are useful for applications to the hypersonic control of vehicles moving through the atmosphere. The purpose of the present study has been to obtain a qualitative and quantitative description of the flow field generated by the two interacting streams; in particular to determine the main parameters governing the flow field and their influence on the penetration and the interaction phenomena. An experimental investigation has been conducted for this purpose and a flow field model developed. The results of the theoretical analysis based on this model are compared with the experimental data.

II. DESCRIPTION OF THE PHYSICAL PHENONEMA

A. Qualitative Observations Concerning the Flow Field Configuration

The flow field resulting from the upstream injection through a wall slot on a forward facing step, incorporates several characteristics of simpler flow fields,

namely:

i) the flow field produced by a free jet issuing into a supersonic counter main stream,

ii) the flow field produced by a forward facing step in a supersonic stream.

In the first case (e.g. Ref. 1) the main features of the flow are a bow shock across which the main stream decelerates on an interface that separates the jet flow from the main flow and, if the jet is supersonic, a second shock system associated with the injectant. In the second case (e.g. Ref. 2) a dividing streamline separates the dead water region that forms in front of the step from the main flow. A mainstream shock is associated with the shape of the dividing streamline.

In the present investigation, the phenomena can be seen to incorporate some of the features of the above flow fields. The flow field resulting from the upstream injection along a wedge wall into a supersonic (Mach 6) main stream is illustrated with shadowgraph pictures and explanatory sketches of the flow field in Fig. 1 for a subsonic jet and in Fig. 2 for a supersonic jet. Typical pressure and temperature distributions for both cases are also shown in Figs. 1 and 2.

The boundary layer separates, as in case (ii) since the main stream has to overcome a large adverse pressure gradient generated by the injected flow and by the step which, together act as an obstruction to the main stream. The injected flow is separated from the main stream, as in the case (i) by a dividing streamline whose position is determined by the condition of equal pressures on both sides at the stagnation point. The jet total pressure is decreased to the value on the dividing streamline by the dissipative effect of viscosity. The viscous dissipation occurs not only through the mixing and the shock (if the jet is supersonic) as in the upstream free jet case, but also through the effect of the

boundary layer on the wall.

B. Flow Field Models and Governing Parameters

The physical phenomena illustrated above can be schematically represented by the flow field models sketched in Figs. 1 and 2. In the subsonic case (Fig. 1) the injected flow decelerates through the action of mixing. The pressure being approximately constant as shown by the present experiments. The jet flow mixes initially with the co-flowing stream of the recirculation region generated by the step in the injection system, and then with the primary flow. The jet flow reverses because of the difference in momentum and mass flow in the direction of the main stream. The distance needed to dissipate through mixing the jet kinetic energy (i.e. the penetration of the jet) increases with the jet total pressure. If the jet is supersonic (Fig. 2) a shock system forms to permit the jet stream to flow in the opposite direction. The jet's kinetic energy dissipation and the shock boundary layer interaction induce a turning of the streamlines, impeding the injected gas from penetrating relatively large distances along the wall. The ensuing expansion gives rise to a reverse flow that has a radius of curvature proportional to the jet Mach number. A large radius of curvature produces a bow shock in front of the reverse flow which increases the shape of the main shock, (i.e. the interaction between the two streams). In both cases the main stream has to overcome the obstacle presented by the secondary jet and its boundary layer separates because of the adverse pressure gradient. The separated region of the main stream exchanges momentum by mixing with the injected flow which is also separated near the dividing streamline.

These qualitative observations suggest that the important parameters governing the structure of the flow field are:

- a) the kinetic conditions of the two streams and their reference Reynolds

number.

b) the mass flow ratio or mixing parameter $\lambda = \frac{\rho_j U_j}{\rho_e u_e}$

c) the geometrical parameters $d_1 = \frac{s}{\ell}$ $d_2 = \frac{\ell}{L}$

III. EXPERIMENTAL INVESTIGATION

A) Description of the Experiments

The experiments were conducted in a Mach 6 blowdown wind tunnel at New York University Aerospace Laboratory. For this series of experiments, the stagnation pressure was maintained between 1000 to 1200 psia and the stagnation temperature was maintained in the range of 600-900°R. Consequently, Reynolds number of the order of 10^8 were achieved. The model was a two-dimensional wedge instrumented with thermocouples and pressure taps on both surfaces (Fig. 3). It had a slightly blunt leading edge of 1/32" radius. The wedge half-angle was 4° and two 3" wide injection chambers were built above the upper and lower surfaces of the wedge. The injection chambers were designed to have interchangeable nozzles, so as to vary the injection Mach number. A variation of the geometrical parameters s/ℓ and ℓ/L was achieved by the addition of streams that gave different values for the height of the exit section of the nozzle (s) and the height of the step (ℓ). The injectant was air, cooled by liquid nitrogen. The injected air temperature was maintained in the range of 250-350°R. Different values of the parameter λ were obtained by varying M_j and T_j .

The experimental output consisted of tunnel and injection flow conditions, shadowgraph pictures, and static pressure and temperature measurements on the region between the leading edge of the wedge and the injection slot. Heat transfer and adiabatic temperature values were also computed by the transient method (Ref. 3) from the temperature distribution in time. The transient method requires that the thermocouples to be on the inside surface of a thin shim mounted flush to the

wedge surface. Corrections were made to overcome the effects of heat conduction within the shimstock to which the thermocouples are attached.

B) Presentation and Discussion of the Results

Diagrams of the measured and reduced quantities are presented here as functions of the position coordinates normalized by the distance L between the slot and the wedge leading edge. A few typical distributions are shown in Figs. 4 and 5 for different injection conditions. The pressure distribution shows the classical trend of boundary layer separation regions and downstream of the reattachment, a second larger plateau, corresponding to the mixing region of the two counterflowing streams. The adiabatic wall temperature distribution shows a smooth decrease in value in the recirculation region of the jet, from that upstream of the separation point. The temperature decrease is steeper in the first pressure plateau region where the wall begins to be influenced by the jet stream stagnation temperature.

As stated previously, two physical quantities which are of relevant significance in determining the flow field structure are the penetration distance and the degree of interaction between the two streams. The penetration distance was determined from a combined observation of the following experimental output:

- a. pressure distribution - by the region of the first pressure plateau
- b. adiabatic wall temperature distribution - by the point where the adiabatic wall temperature drops rapidly from the mainstream value
- c. shadowgraph pictures - by the point where the dividing streamline intersects the body surface.

The degree of interaction of the jet stream with the mainstream was determined from:

- a. the pressure change $\left(\frac{\Delta p}{p_0}\right)$ corresponding to the large plateau, produced by the injection

b. the slope and therefore the strength of the coalesced shock formed by the bow and the separation shocks.

The variation of the penetration distance and of the degree of interaction, as determined by the above criteria, with the jet Mach number are illustrated in Fig. 6. The penetration is proportional to the total momentum when the jet is subsonic or low supersonic. For the latter this conclusion holds if the height of the jet is sufficiently small compared to the mixing length, so that the supersonic injectant flow becomes subsonic by viscous mixing dissipation without a local shock. If the jet is supersonic and a jet shock is present, the penetration decreases, as discussed in Section 2, while the interaction increases. For cooling applications, the dependence of the penetration distance on the geometric parameters s/ℓ and ℓ/L and on the mixing parameter λ , is best correlated by the cooling effectiveness γ , defined as a function of the adiabatic wall temperature

$$\gamma = \frac{T_{aw} - T_{\infty}}{T_{oj} - T_{\infty}}$$

The variation of γ was determined as a function of a new parameter, χ defined as the product of powers of the main parameters

$$\chi = \left(\frac{x}{s}\right)^{0.75} (\lambda)^{-1.5} \left(\frac{s}{\ell}\right)^{0.45} \quad (1)$$

The exponents in the above expression were determined (Ref. 4) from logarithmic plots of γ versus each parameter at constant values of the other two. Plotting γ in this new defined variables, a straight line correlation is obtained (Fig. 7)

$$\gamma = C - K \chi$$

The validity of the suggested correlation extends over the complete range of the measured values. The above correlation indicates the possibility of using the

upstream injection scheme for cooling purposes. Particularly interesting, from a technical point of view, is the application of this scheme to the leading edge cooling of a body in a supersonic stream, when the total pressure losses through the bow shock must be maintained relatively small. A study of this application is presented in detail in Ref. 4.

IV. THEORETICAL ANALYSIS

A. General Considerations

Following the flow field model described in Section 2, the mixing between the two counterflowing streams essentially governs the structure of the flow field under consideration, if the upstream jet is subsonic or low supersonic. This case is particularly important when high jet penetration is desired, as in the case for cooling applications.

The mixing region of the flow field model is amenable to theoretical analysis if the usual boundary layer approximations are assumed to be valid. The pressure can also be assumed constant in the region of interest, as inferred by the experimental observations (Section 3). With these assumptions, the mixing region of the flow field is governed by the conservation equations for turbulent compressible boundary layer with zero pressure gradient

$$\begin{aligned} \frac{\partial \rho u}{\partial x} + \frac{\partial \rho v}{\partial y} &= 0 \\ \rho u \frac{\partial u}{\partial x} + \rho v \frac{\partial u}{\partial y} &= \frac{\partial}{\partial y} \left(\rho \epsilon \frac{\partial u}{\partial y} \right) \\ \rho u \frac{\partial H}{\partial x} + \rho v \frac{\partial H}{\partial y} &= \frac{\partial}{\partial y} \left(\rho \epsilon \frac{\partial H}{\partial y} \right) \end{aligned} \quad (2)$$

The flow field in the mixing region is essentially nonsimilar because of the jet velocity decay in the upstream direction. A locally similar analysis was conducted by combining:

1. a nonsimilar solution essentially valid near the wall in the jet region, which takes into account the upstream velocity decay of the jet flow field.

2. a station by station similar solution dependent on the local external stream conditions

B. Solution

The locally similar solution is considered first. Under the similarity assumption, the new dependent and independent variables are introduced in the usual way (Ref. 5)

$$\eta = \frac{y}{x} \epsilon_0^{-\frac{1}{2}}$$

$$f = \int_0^n \frac{\rho u}{\rho_1 u_1} dn \quad (3)$$

$$\psi = \rho_1 u_1 x \epsilon_0^{\frac{1}{2}} f(\eta)$$

where the subscript 1 and 2 denote the higher and lower momentum external streams and x is measured from the upstream penetration point. In the previous definitions the eddy viscosity is assumed to be proportional to x through a factor ϵ_0 which is different for different eddy viscosity models.

In these variables, using the Crocco integral of the energy equation, the unknown function $\bar{u} = \frac{u}{u_1}$ and $g = \frac{t}{t_1}$ are determined from the following system of equations.

$$\bar{u} = gf'$$

$$g\bar{u}'' - g' \bar{u}' + g^2 \bar{f}u' = 0 \quad (4)$$

$$g = 1 + B(\bar{u}-1) - C(\bar{u}^2-1)$$

where B and C are functions of the external stream properties. The physical problem under consideration is now reexamined in order to define the appropriate

boundary conditions for the ordinary differential equations system (4). The wall boundary layer, however determined in the establishment of the flow field configuration, can be neglected in the mixing region calculation, if the height of the injection system is large with respect to the boundary layer thickness in the immediate vicinity of the jet. Assuming this approximation valid, the wall can be considered as a flow field streamline. Two of the three necessary boundary conditions are imposed, as in the case of mixing between coflowing streams, at plus infinity and at the dividing streamline. The dividing streamline can be considered, without loss of generality. The axis $\eta = 0$, and its position determined later on. The two conditions are expressed by

$$u = u_1 \quad \text{for } \eta \rightarrow \infty \quad (5)$$

$$\psi = 0 \quad \text{for } \eta = 0 \quad (6)$$

The third boundary condition is imposed, not at minus infinity as in the case of mixing between coflowing streams, but at a free boundary η_0 determined by the condition that the stream function is again zero. In fact, when mixing occurs between counterflowing streams the lower momentum must be considered finite, since it reverses completely in the direction of the higher momentum stream. The third condition is expressed by

$$u = u_2 \quad \text{for } \eta = \eta_0 \quad (7)$$

where η_0 is determined by the integral condition

$$f = \int_0^{\eta_0} \frac{\rho u}{\rho_1 u_1} d\rho = 0 \quad (8)$$

The ordinary differential equation system was solved numerically with a quasi-linearization technique (Ref. 6). Numerical results are shown in Figs. 8, 9, and 10 for different ratios of u_1/u_2 . The velocity profiles are different from the coflowing streams case, in particular, they are extended farther in the negative side of the η axis, and consequently also the value of the normal velocity component, v , is larger as can be expected because of the reverse flow. The position of the dividing streamline is finally determined imposing the condition that the position of the wall corresponds to $\eta = \eta_0$. The above similar solution cannot take into account the influence of the initial profile and cannot give the decay of u_j with the upstream distance from the jet. To improve the solution the nonsimilarity of the problem must be kept in the equations that are, however, linearized to obtain an analytical solution. Accordingly, to the improved Oseen linearization (Ref. 7) the momentum or energy equations are reduced to the form

$$(\rho u)^* \frac{\partial p}{\partial x} = \frac{\partial}{\partial y} \left(\rho \epsilon \frac{\partial p}{\partial y} \right) \quad (9)$$

where $(\rho u)^*$ is an approximate average value determined in such a way that the approximation gives the minimum error, and the symbol p indicates either velocity or total enthalpy. With the hypothesis that $\rho \epsilon$ is only a function of x , the Eq. 9 can be reduced to the heat transfer equation form

$$\frac{\partial p}{\partial \xi} = \frac{\partial^2 p}{\partial y^2} \quad (10)$$

where the variable ξ is defined as

$$\xi = \int_0^x \frac{\rho \epsilon}{(\rho u)^*} dx \quad (11)$$

The initial condition is specified differently for the total enthalpy and for the velocity field

$$p(\partial, y) = w(\partial, y) \quad (12)$$

and the boundary conditions are

$$p = p_e \quad \text{for } y \rightarrow \infty \quad (13)$$

$$\frac{\partial p}{\partial y} = 0 \quad \text{for } y = 0 \quad (14)$$

The last condition is valid for the velocity field solution in the hypothesis, previously made, that the wall boundary layer is neglected and the wall is a streamline (in particular a centerline streamline). For the total enthalpy field solution the adiabatic wall condition (14) approximately represents the present experimental conditions (thin skinned model) and therefore is the more appropriate to compare the present calculations with the experimental results. The solution of the equation (10) and boundary conditions (12, 13 and 14) and be expressed in the form (Ref. 8).

$$p(\xi, y) = p_e + \int_0^{\infty} [w(y') - p_e] G(y, y', \xi) dy'$$

where the Green function $G(y, y', \xi)$ associated with the system is given by

$$G(y, y', \xi) = \frac{1}{2\pi\xi} \left[\exp\left(-\frac{(y+y')^2}{2\xi^{1/2}}\right) + \exp\left(-\frac{(y-y')^2}{2\xi^{1/2}}\right) \right]$$

Results for particular values of the initial velocity and total enthalpy profiles are reported in Ref. 4. An appropriate value of $(\rho u)^*$ must be defined in order to return from the transformed plane (ξ, y) to the physical plane (x, y) the value

$$(\rho u)^* = \rho_j u_j(x)$$

was adopted to have good approximation in the jet region. This linearized solution is not strictly valid far away from the jet region, therefore it was

used only as a guide in selecting the similar profile valid at each particular axial station, by matching the u_1 of the similar solution with the velocity $u(x,0)$ of the nonsimilar solution. In this way the nonlinearity of the original equations is retained through the similar solution, and the local similarity concept is applied to describe station by station, the entire mixing region of the flow field.

C. Results

Numerical results for this solution were calculated with the eddy viscosity model suggested in Ref. 9. As an example, the velocity flow field, consisting of the velocity profiles and the dividing streamline, in one particular condition, is shown in Fig. 11. The flow field structure is well reproduced (from a qualitative point of view). The agreement with the experimental results is fairly good for the shape of the dividing streamline while the penetration length is not predicted as well (Fig. 11). The theoretically predicted cooling effectiveness, and therefore the wall temperature, is shown in Fig. 12 as a function of the parameter χ defined in (1). The predictions compared with the experimental measured values are in good agreement in the range $30 \leq \chi \leq 70$.

The discrepancies between the experimental results and the theoretical model are due to the approximations adopted. The flow in the region of the dividing streamline near the wall is much more complex than it has been assumed in the analysis. The theoretical model can be improved by considering the effect of the wall boundary layer neglected in this analysis and possibly using an eddy viscosity model more appropriate to this problem. However, the model provides a very simple means of predicting the flow field's major features in a satisfactory way.

V. CONCLUSIONS

The flow field resulting from the interaction of an upstream facing wall jet with a supersonic counterflowing stream, has been studied. An experimental investigation has been conducted to clarify the physical phenomena and to determine the flow field characteristics for different ranges of the main parameters. A flow field model was determined from the experimental observations for both subsonic and supersonic jet conditions. The jet penetration distance and the degree of interaction between the two streams are the most relevant physical quantities in the determination of the flow field structure. The results show:

- a. large penetration distances in the case of high subsonic or low supersonic jet,
- b. large interaction forces for higher supersonic injections.

In the first case the mixing between the two counterflowing streams essentially governs the flow field configuration. A theoretical analysis was performed to study this region. The theoretical predictions, obtained by applying a locally similar solution, reproduce the flow field's major features in a satisfactory way. The cooling effectiveness correlated as a function of a product of powers of the main parameters, suggests the possibility of the use of the upstream injection scheme for cooling applications.

ACKNOWLEDGEMENT

This report was prepared under the National Aeronautic and Space Administration, under Grant No. NGR-33-016-131. The author wishes to thank Dr. Antonio Ferri for suggesting this research and for his guidance during the progress of the investigation.

REFERENCES

1. Romeo, David, J. and Sterrett, James, R., "Exploratory Investigation of the Effect of a Forward Facing Jet on the Bow Shock of a Blunt Body in a Mach Number 6 Free Stream," NASA TND-1065, 1963.
2. Bogdonoff, S.M. and Kepler, C.E., "Separation of a Supersonic Turbulent Boundary Layer," Report 249, Princeton University, Department of Aeronautical Engineering, January 1954.
3. Zakkay, Victor, Sakell, L., and Parthasarathy, K., "An Experimental Investigation of Supersonic Slot Cooling," Proceedings of the 1970 Heat Transfer and Fluid Mechanics Institute, Stanford University Press, Stanford, California.
4. Piva, R., "Leading Edge Cooling by Upstream Injection," NASA CR-111965, December 1971.
5. Napolitano, L.G., Libby, P.A., and Ferri, A., "Recent Work on Mixing at the Polytechnic Institute of Brooklyn," PIBAL 435, December 1957.
6. Kalaba, R., "Some Aspects of Quasilinearization," Nonlinear Differential Equations and Nonlinear Mechanics, edited by J.P. LaSalle and S. Lipschitz (Academic Press Inc., New York, 1963).
7. Lewis, J.A. and Carrier, G.F., "Some Remarks on the Flat Plate Boundary Layer," Journal of Applied Mathematics, Vol. II, No. 2, 1949.
8. Carslaw, H.S. and Jaeger, J.C., "Conduction of Heat in Solids," Oxford Press, 1967.

9. Ferri, A., Libby, P.A., and Zakkay, V., "Theoretical and Experimental Investigation of Supersonic Combustion," ARL Report 62-467, September 1962.



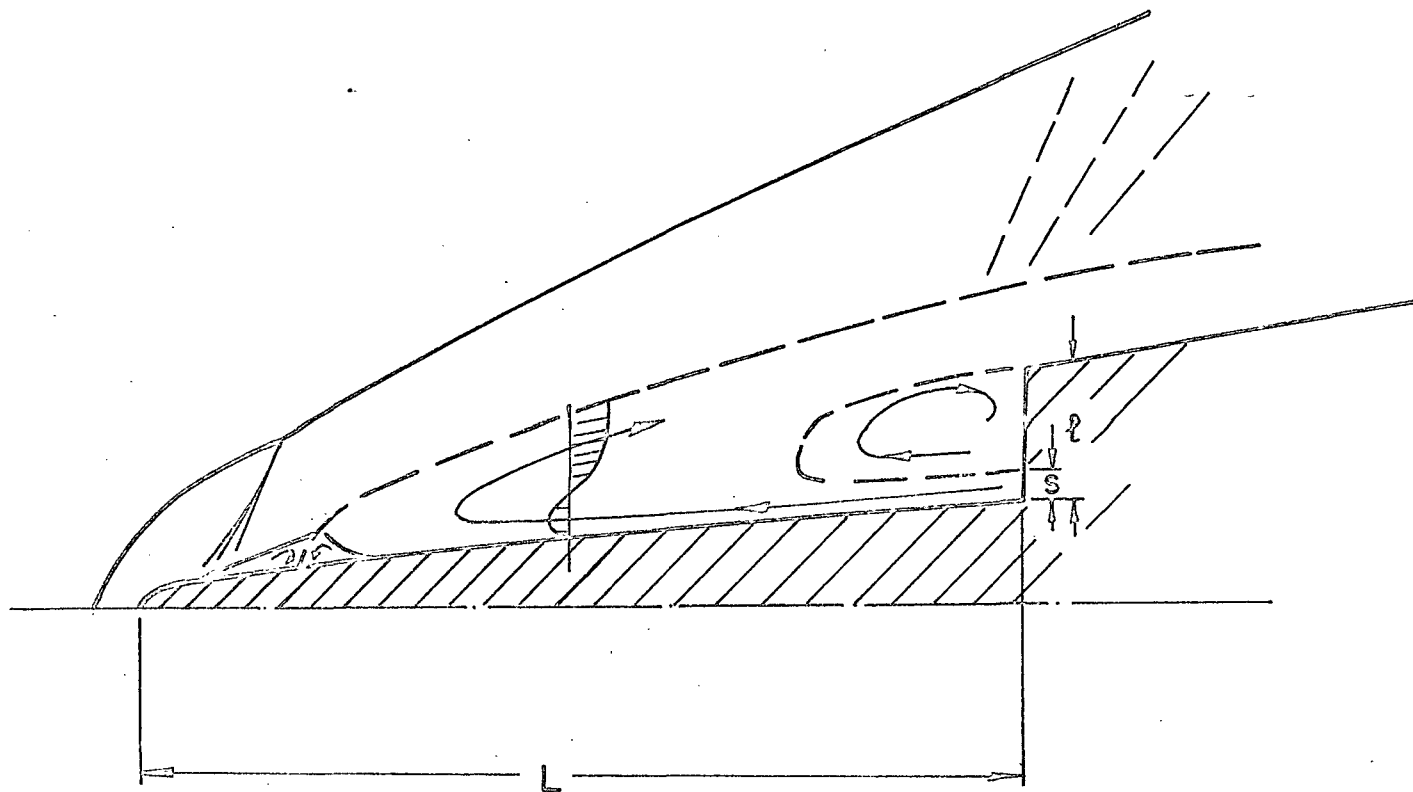
High Subsonic Injection

Reproduced from
best available copy. 



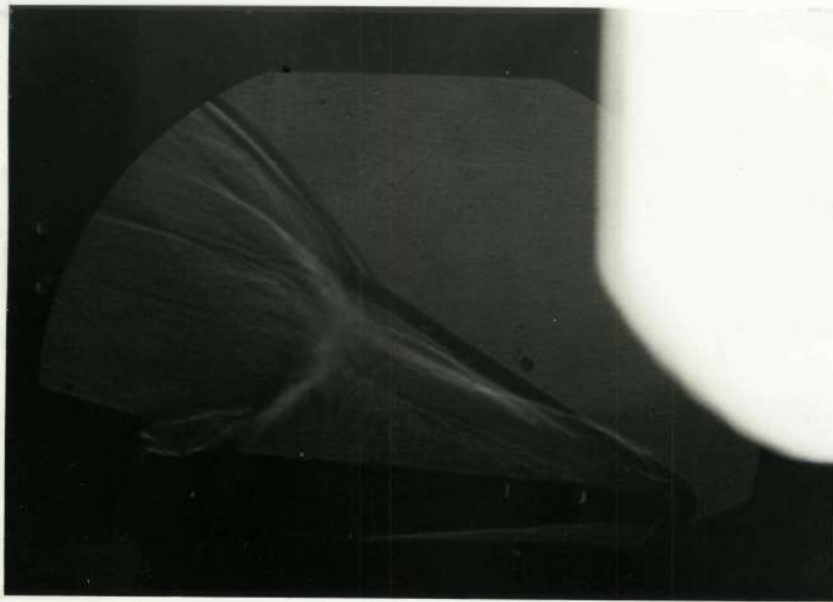
Low Subsonic Injection

Fig. 1a Shadowgraph pictures: Sunsonic Injection



UPSTREAM INJECTION FLOW FIELD

Fig. 1b Flow field produced by upstream injection along the wall; subsonic injection



High Supersonic Injection

Reproduced from
best available copy. 



Low Supersonic Injection

Fig. 2a Shadowgraph pictures: Supersonic Injection

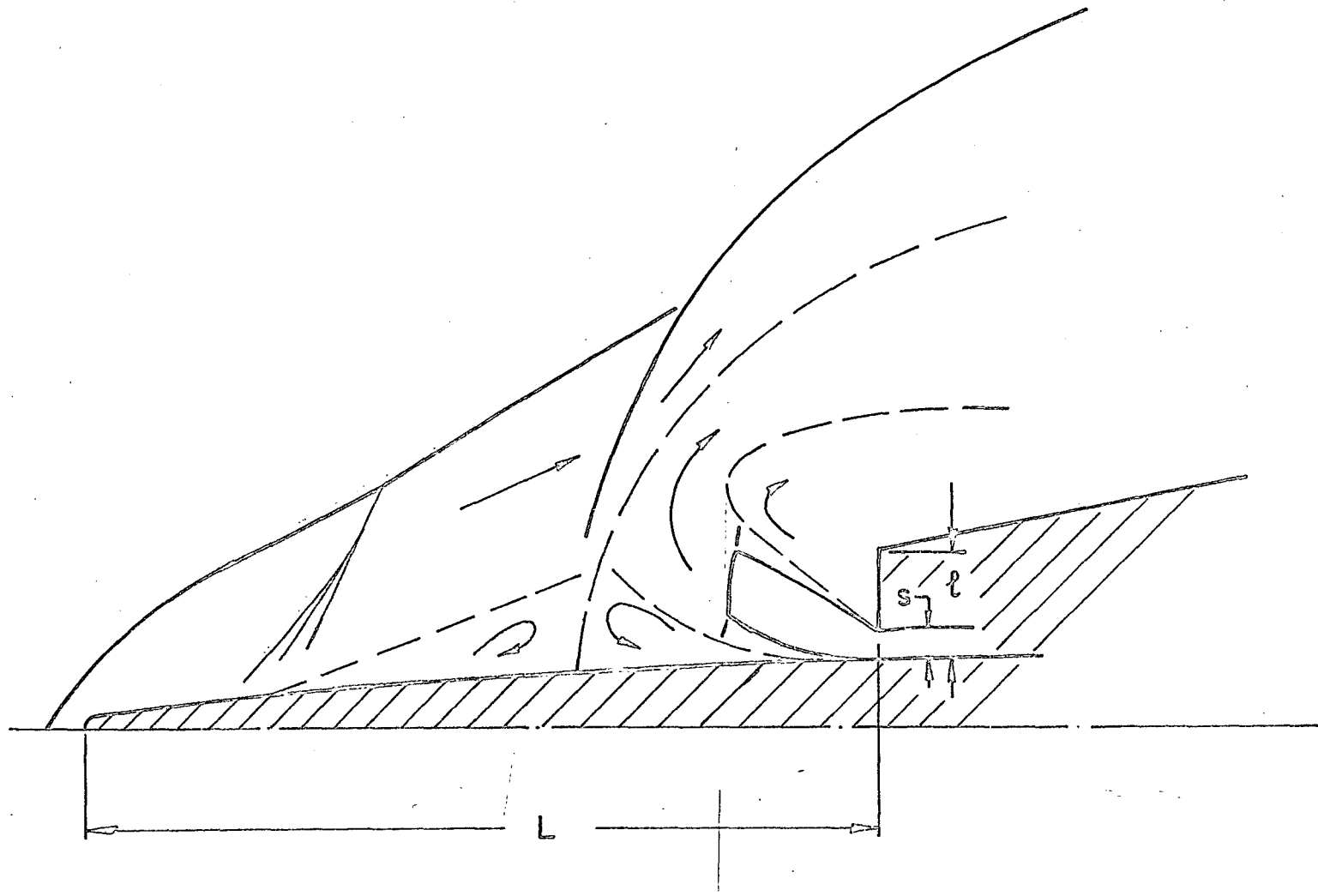


Fig 2b Flow field produced by upstream injection along the wall: supersonic injection

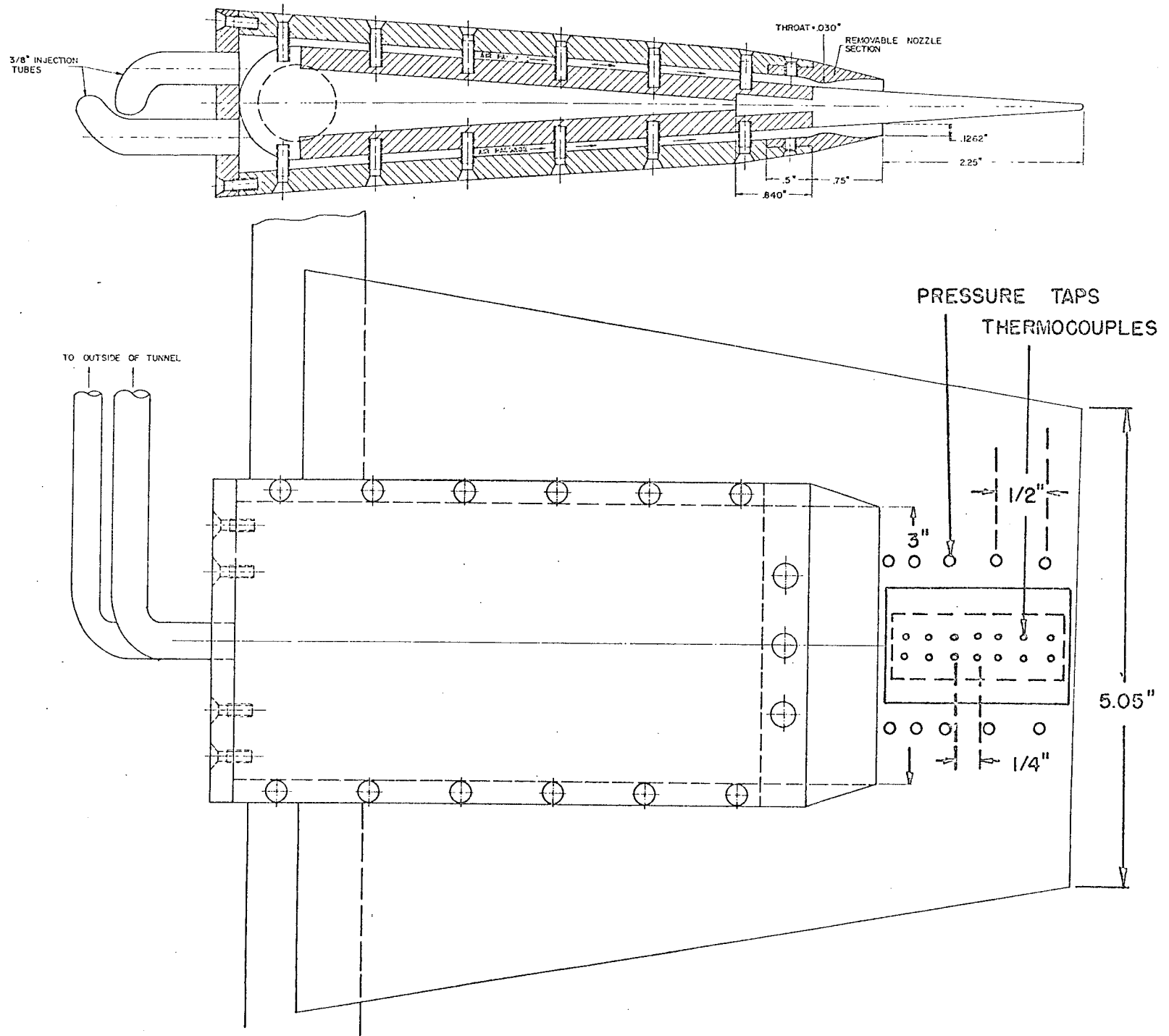


Fig 3 Experimental model

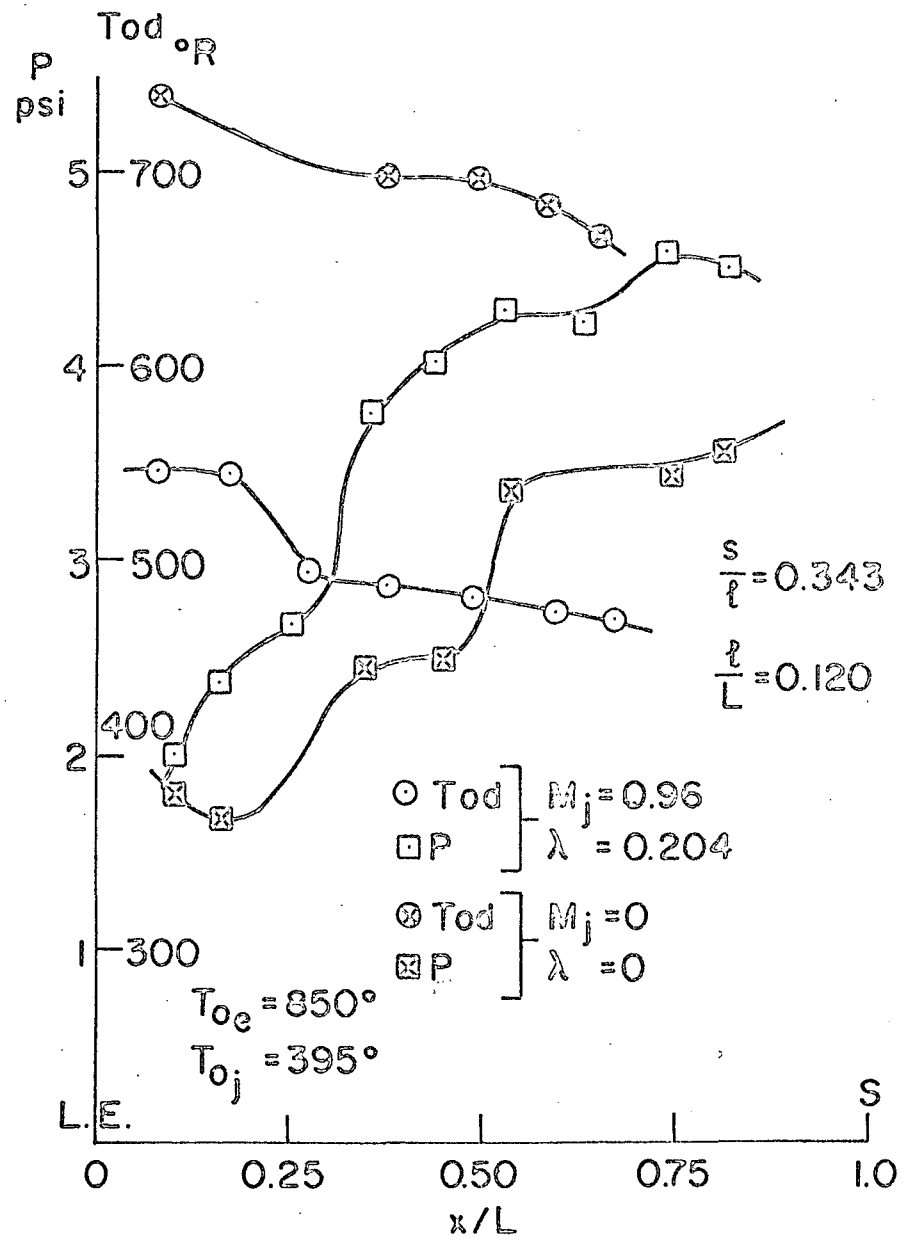
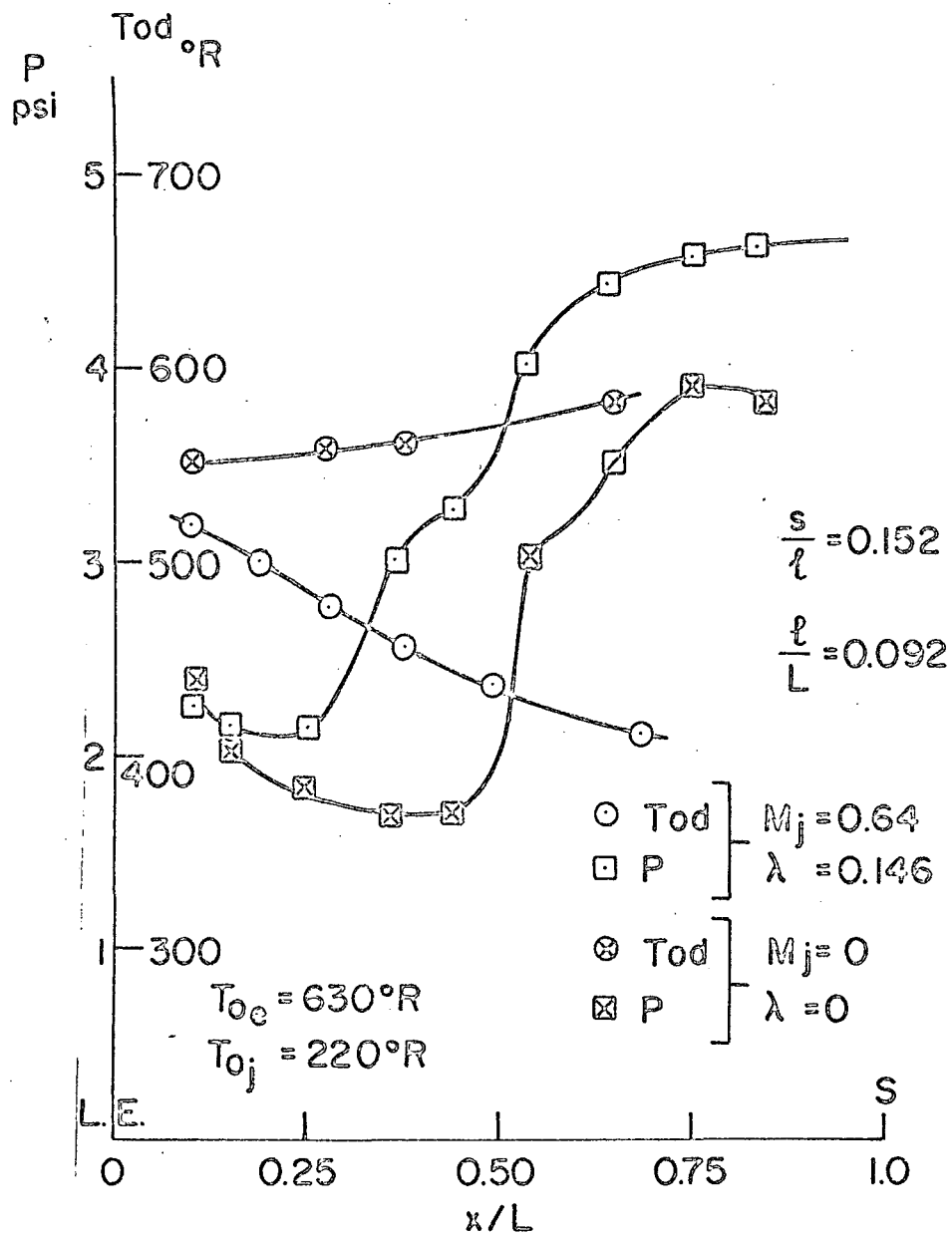


Fig 4 Description of the measured quantities along the wall between the leading edge and the injection slot: subsonic injection

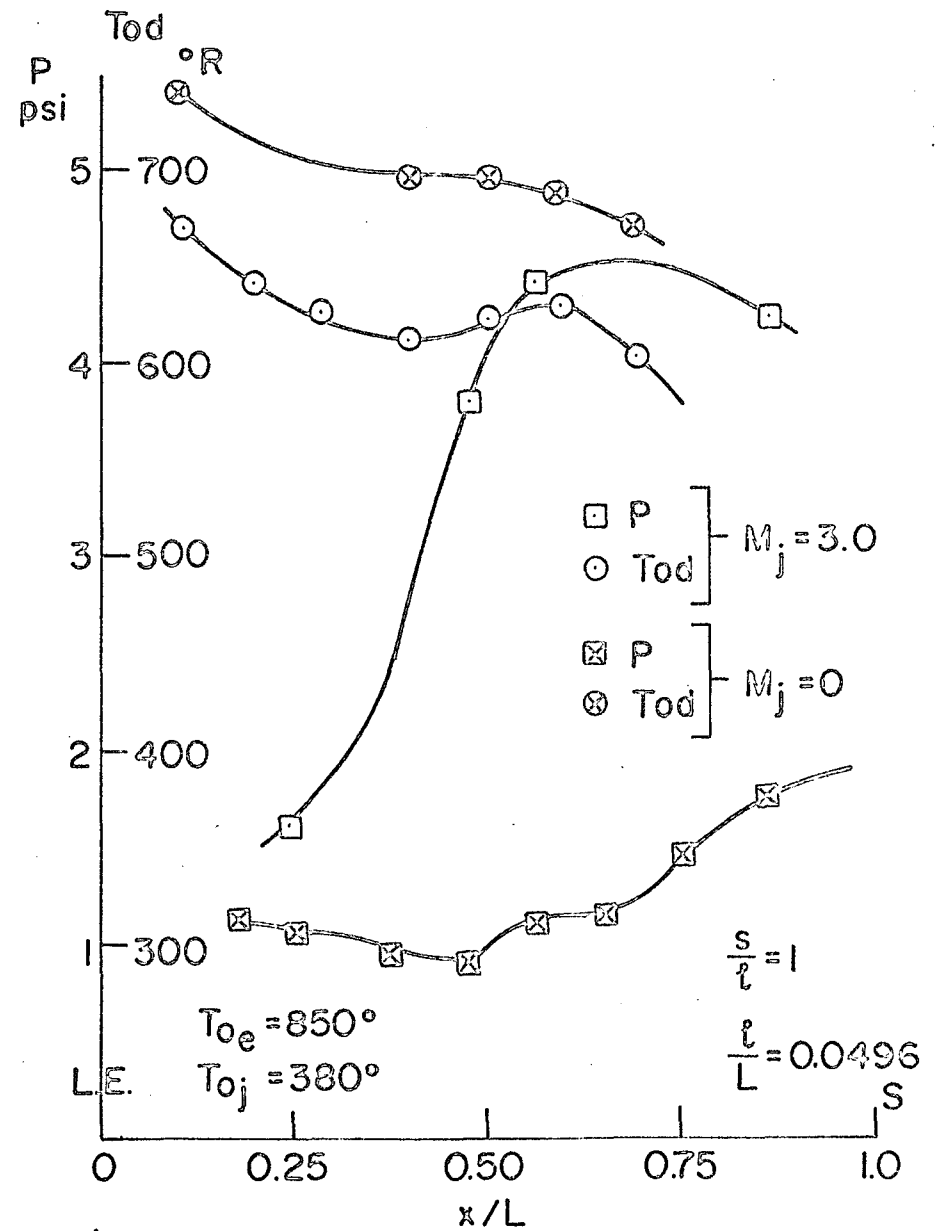
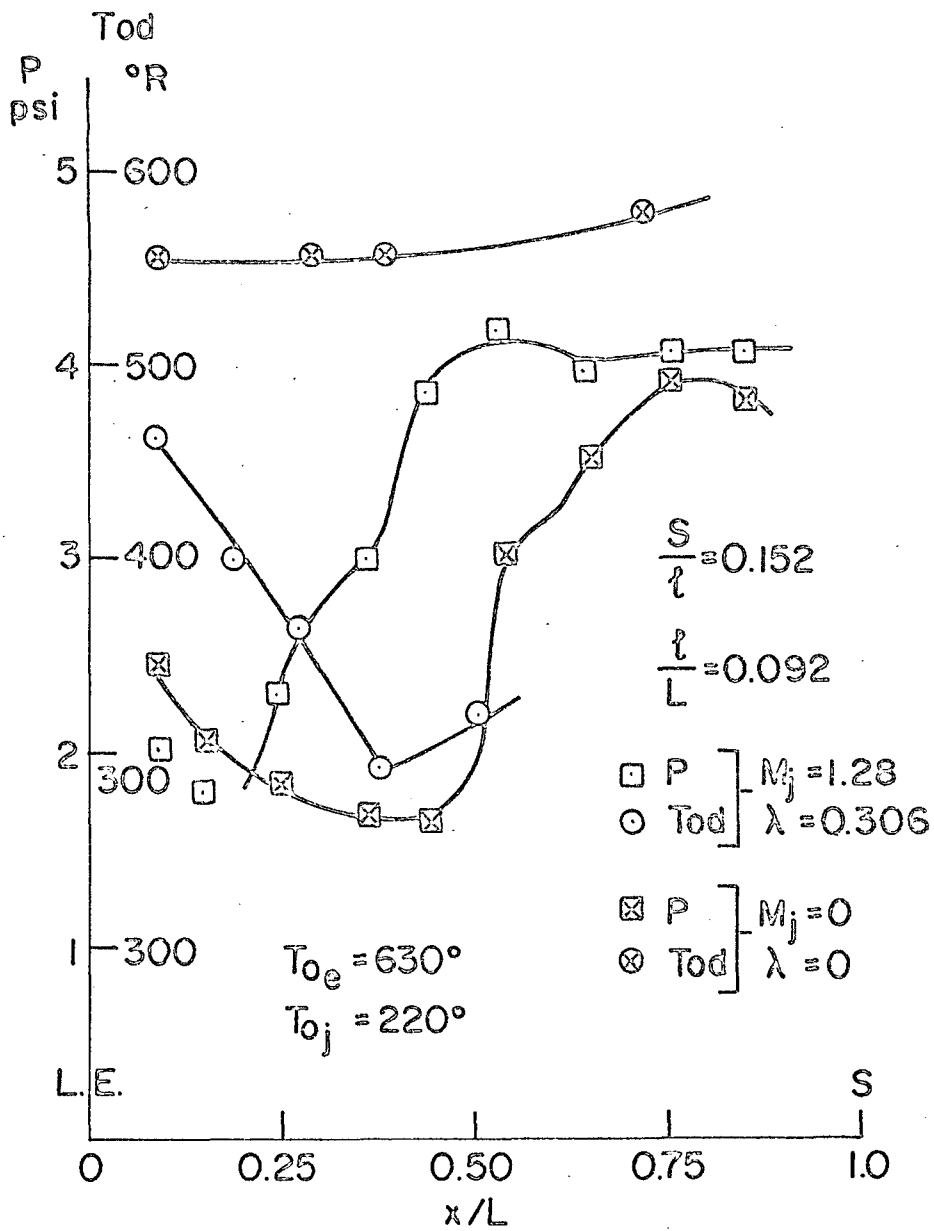


Fig. 5 Distribution of the measured quantities along the wall between the leading edge and the injection slot: supersonic injection

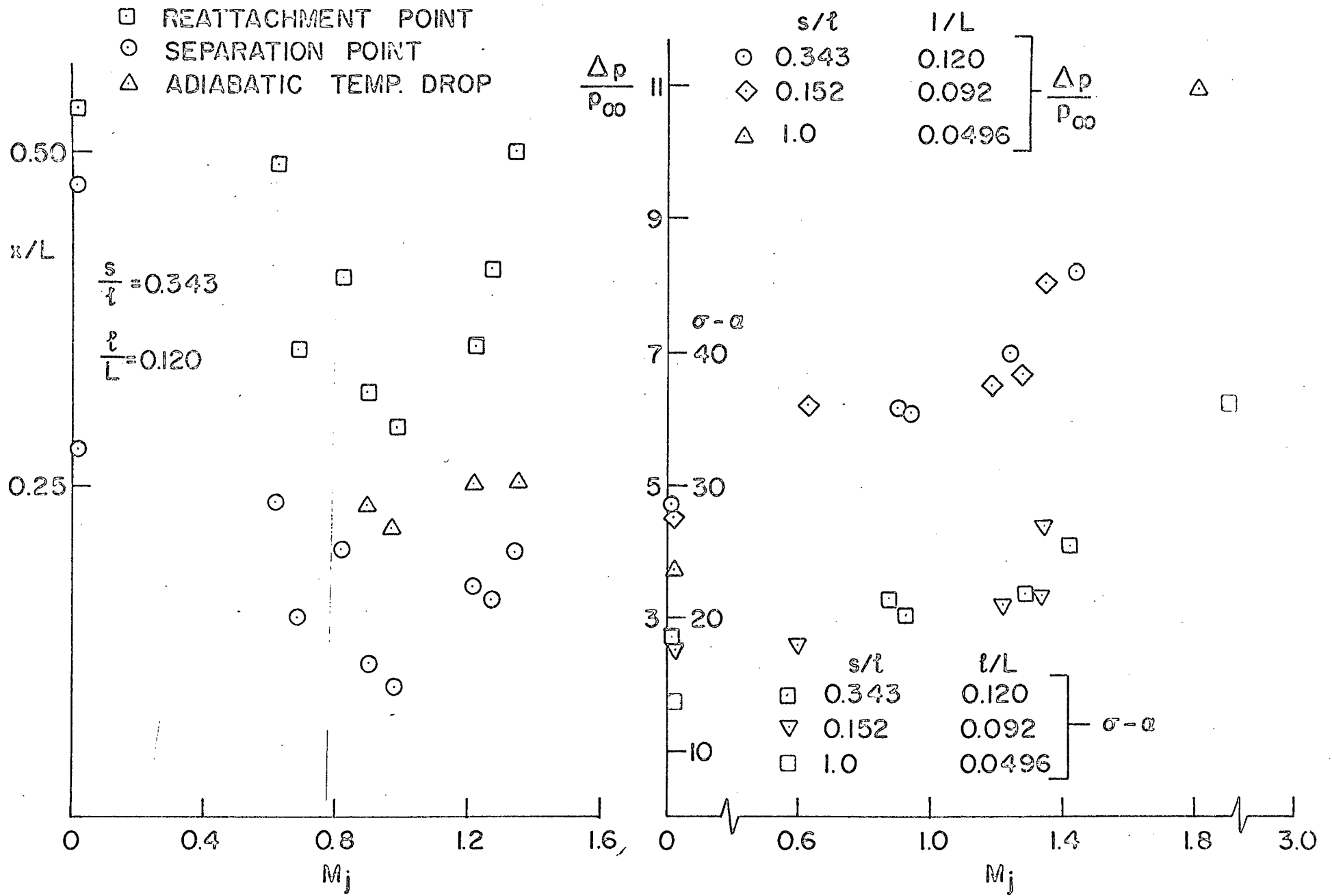


Fig. 6 Measured quantities indicative of jet penetration and interaction, vs jet Mach number

$\frac{T_c - T_{c0}}{T_{c0} - T_{c1}}$
 $\frac{T_c - T_{c0}}{T_{c0} - T_{c1}}$

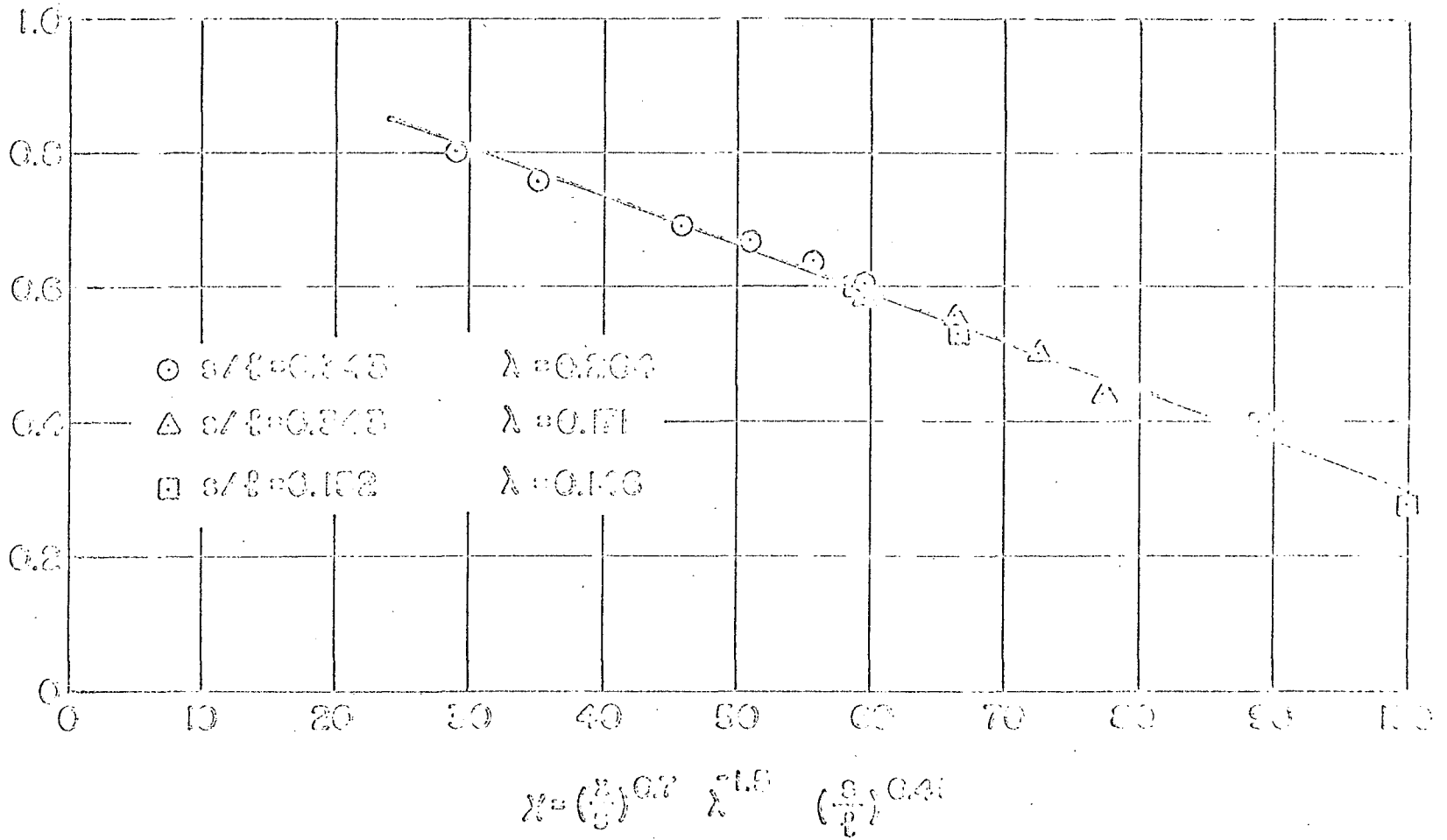


Fig. 7 Cooling effectiveness correlation

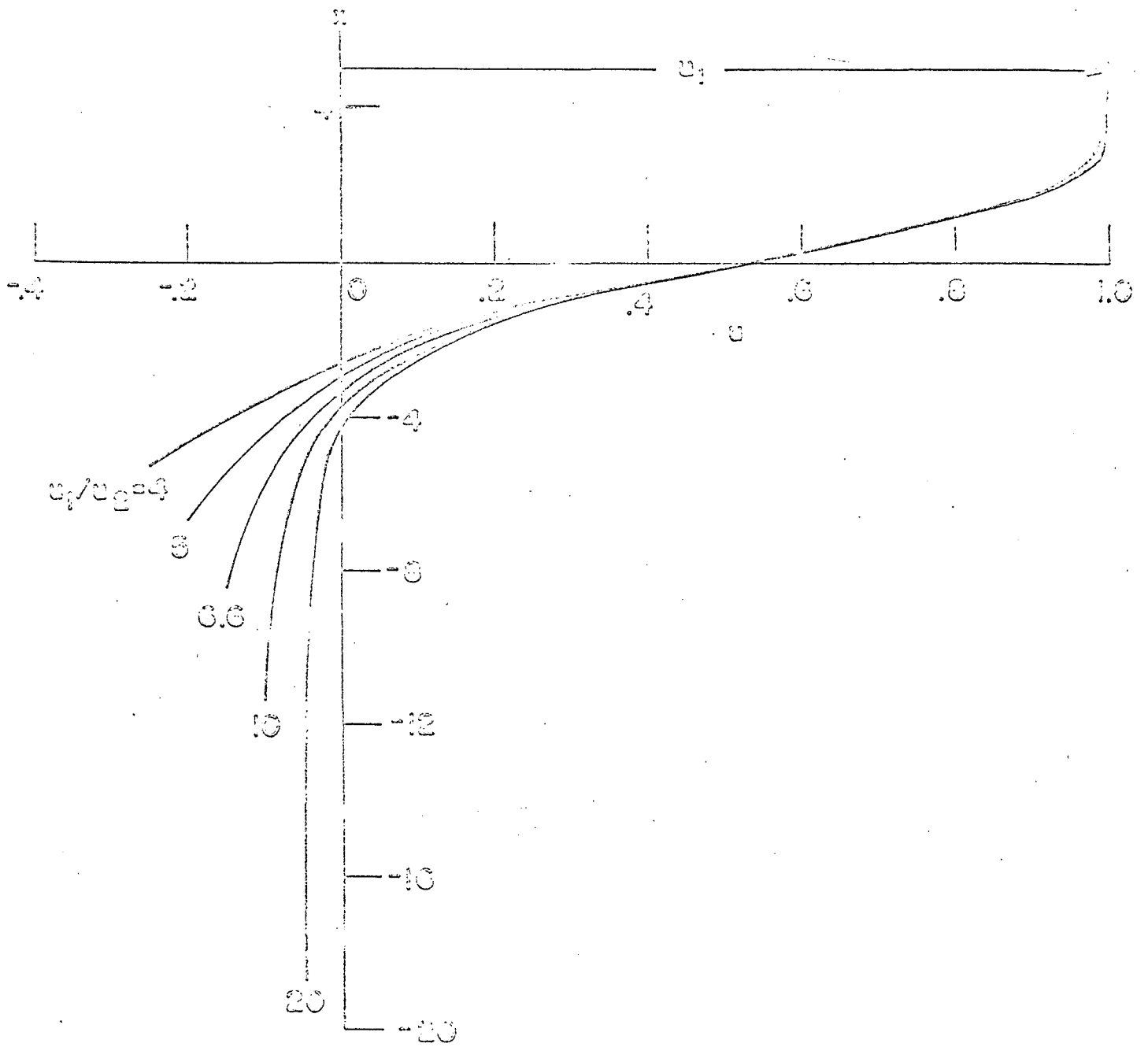


Fig. 8 Similar solution; nondimensional velocity profiles

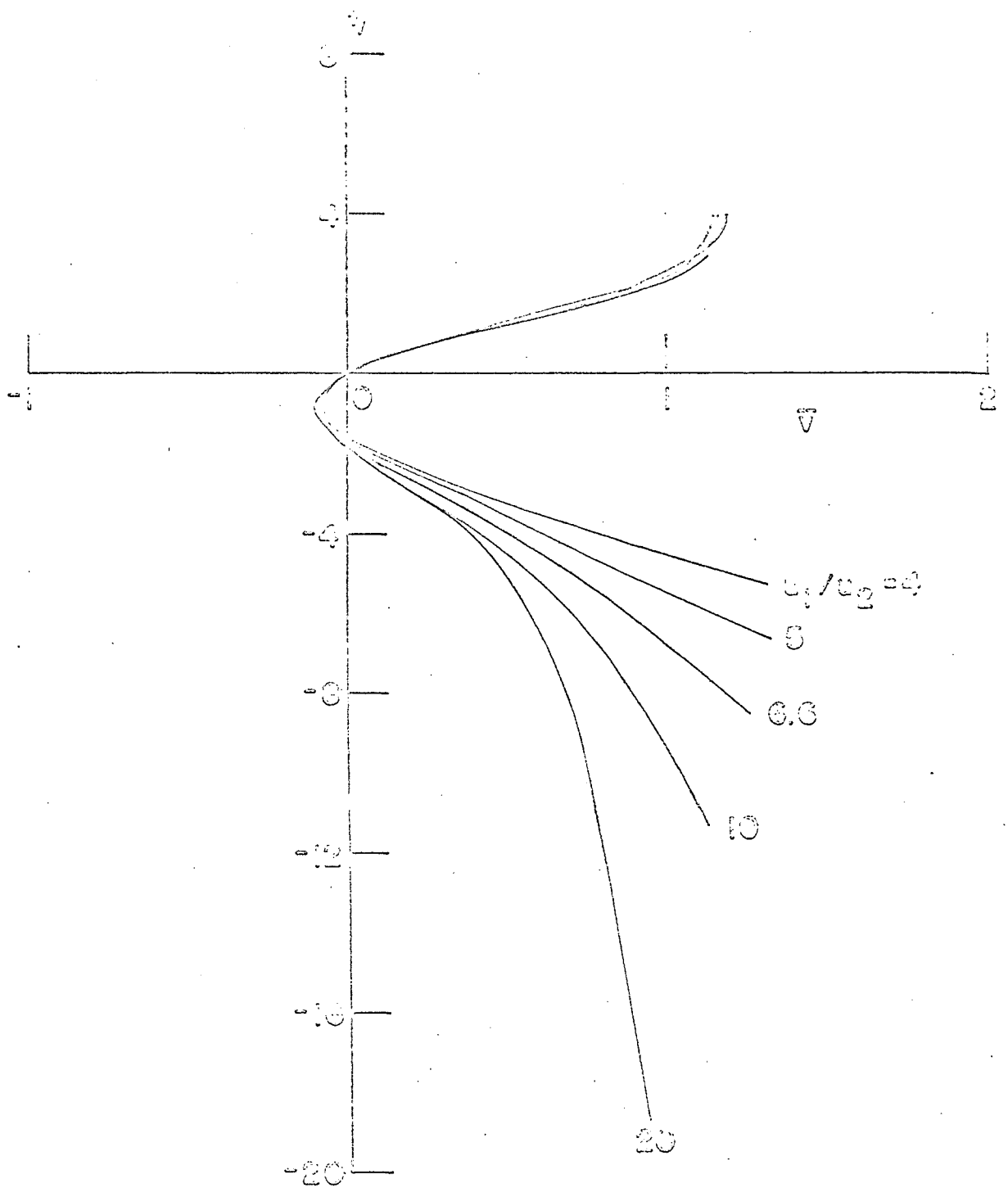


Fig. 9 Similar solution; nondimensional normal velocity profiles

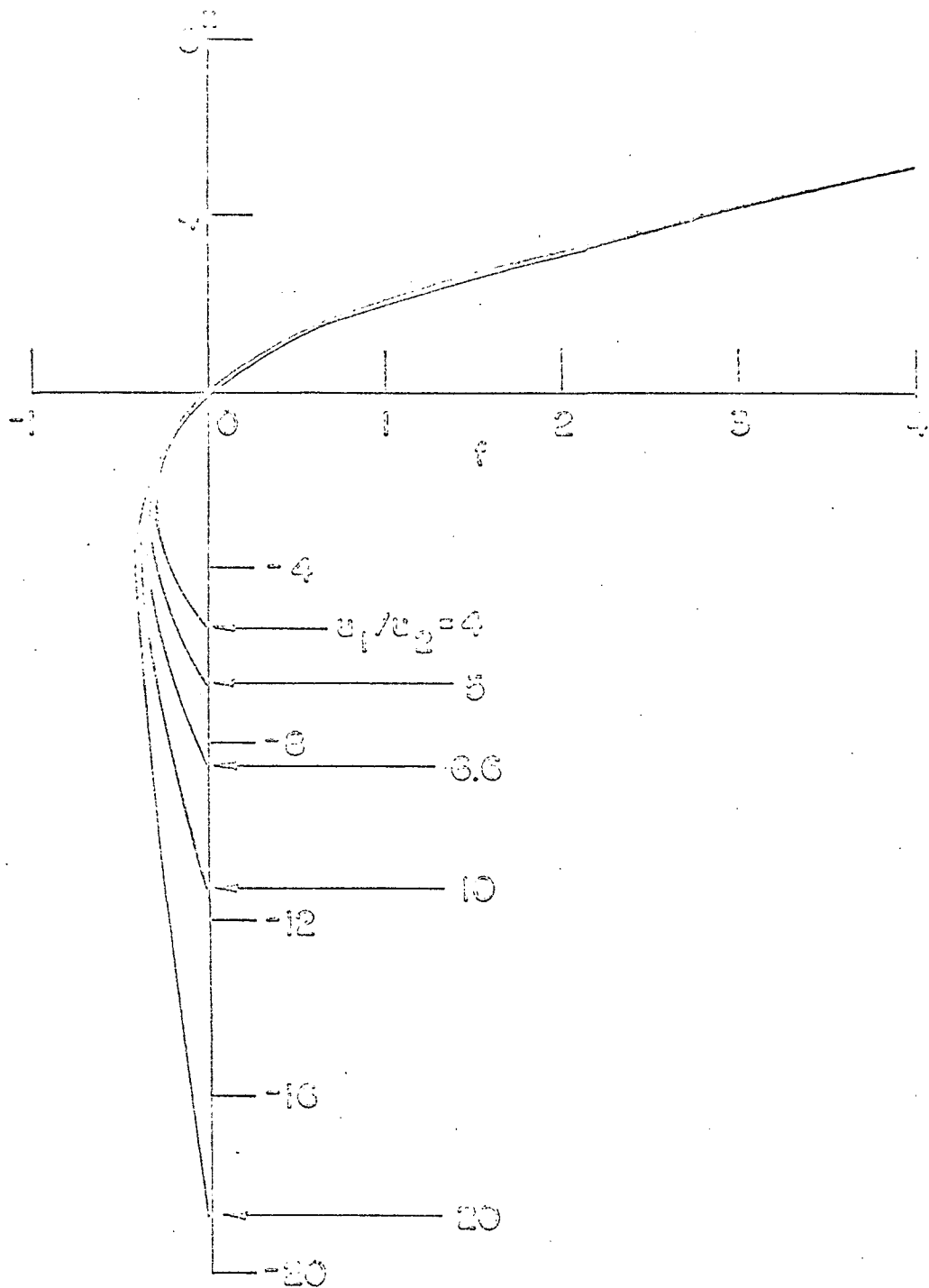


Fig. 10 Similar Solution; nondimensional stream function profiles

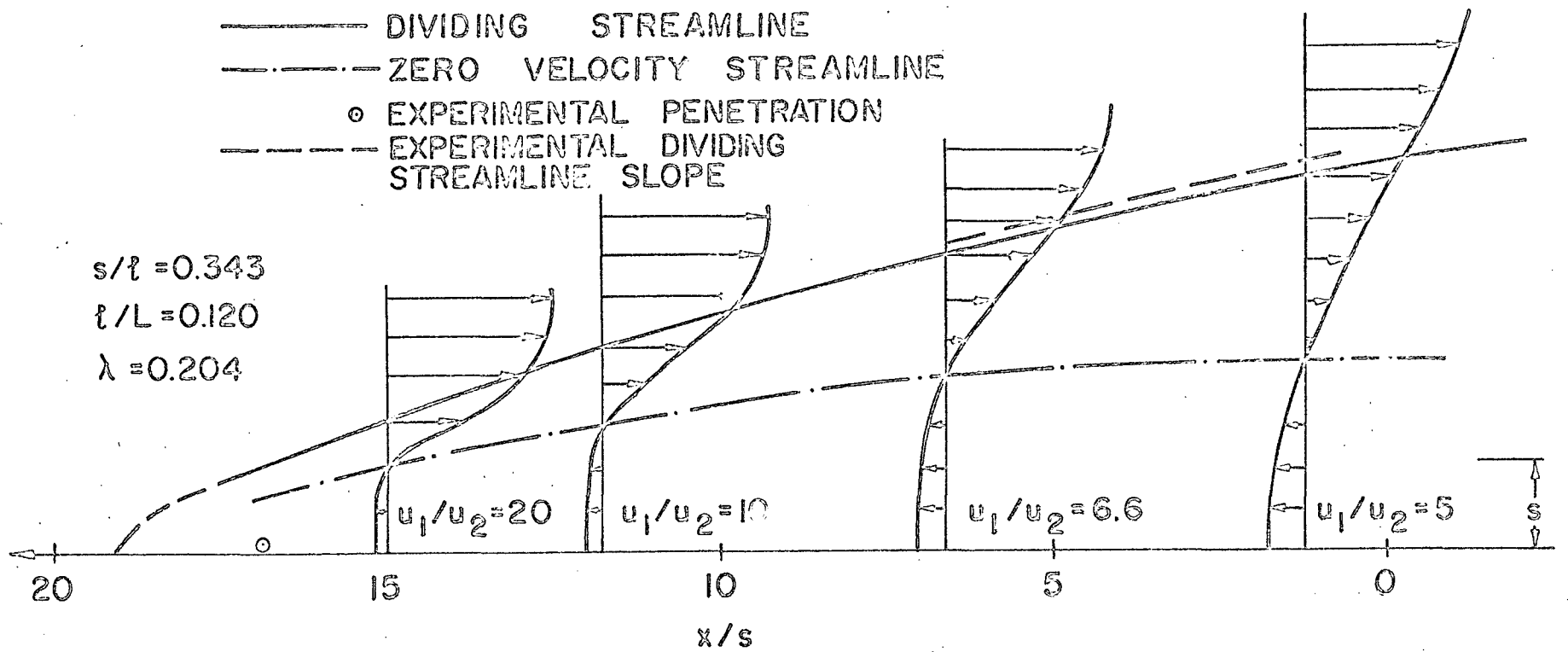


Fig. 11 Locally similar solution

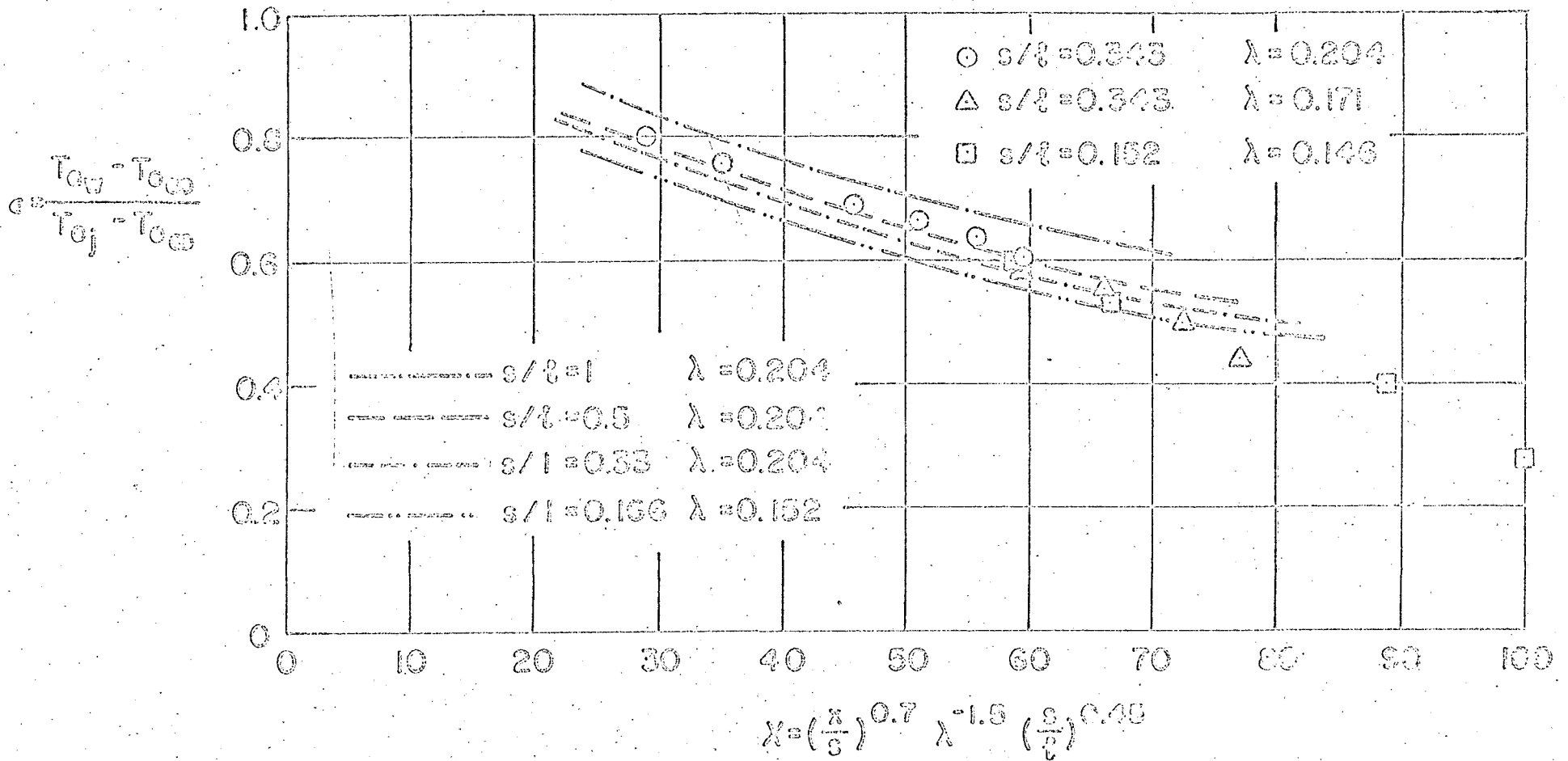


Fig. 12 Comparison of theoretical and experimental cooling effectiveness